AD-A093 630 WISCONSIN UNIV-MADISON MATHEMATICS RESEARCH CENTER F/G 12/1
SOLUTION OF PACKED-BED HEAT-EXCHANGER MODELS BY ORTHOGONAL COLL--ETC(U)
SEP 80 A G DIXON DAAG29-80-C-0041
UNCLASSIFIED MRC-TSR-2116 NL

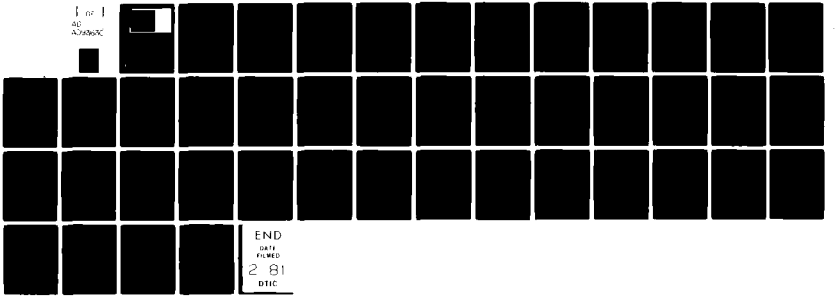

MRC Technical Summary Report #2116

SOLUTION OF PACKED-BED HEAT-EXCHANGER MODELS BY ORTHOGONAL COLLOCATION USING PIECEWISE CUBIC HERMITE FUNCTIONS

A. G. Dixon

Mathematics Research Center
University of Wisconsin—Madison
610 Walnut Street
Madison, Wisconsin 53706

September 1980

(Received June 13, 1980)

Approved for public release
Distribution unlimited

Sponsored by

U. S. Army Research Office
P. O. Box 12211
Research Triangle Park
North Carolina 27709

and

National Science Foundation
Washington, D.C. 20550

UNIVERSITY OF WISCONSIN - MADISON
MATHEMATICS RESEARCH CENTER

SOLUTION OF PACKED-BED HEAT-EXCHANGER MODELS BY ORTHOGONAL COLLOCATION USING PIECEWISE CUBIC HERMITE FUNCTIONS

A. G. Dixon

Technical Summary Report # 2116

September 1980

ABSTRACT

Orthogonal collocation using piecewise cubic Hermite functions is used to solve the elliptic partial differential equations arising from pseudo-continuum models of heat transfer in a packed bed. Problems arising from a discontinuity in the wall boundary condition and from the semi-infinite domain of the differential operator are discussed. Comparison is made between the computed solution and experimental results.

AMS (MOS) Subject Classifications: 65N35, 80A20.

Key Words: Orthogonal collocation, elliptic partial differential equations, Hermite functions, heat transfer in packed beds.

Work Unit Number 2 - Physical Mathematics

Sponsored by the United States Army under Contract No. DAAG29-80-C-0041 and the National Science Foundation under Grant No. ENG76-24368.

SIGNIFICANCF AND EXPLANATION

Models used by engineers are often simplified in the interests of mathematical convenience, rather than in accord with physical reality. A typical case is the omission of axial conduction from models of heat transfer in packed beds, thus allowing an initial-value problem to be solved in the axial direction, instead of a boundary-value problem.

This work demonstrates the application of orthogonal collocation, a numerical method for the solution of differential equations, to packed bed models which include axial conduction. The method is accurate and relatively fast, due to the local nature of the approximating functions used; these make it a good candidate for the solution of "difficult" problems, in which steep gradients are involved.

A formal notation for the method is given, which casts the method in a framework similar to that of the polynomial orthogonal collocation method already familiar in the chemical engineering literature (12, 21). Some tentative suggestions for the implementation of the method are given, in the form of subroutines supplied in an appendix to the main text.

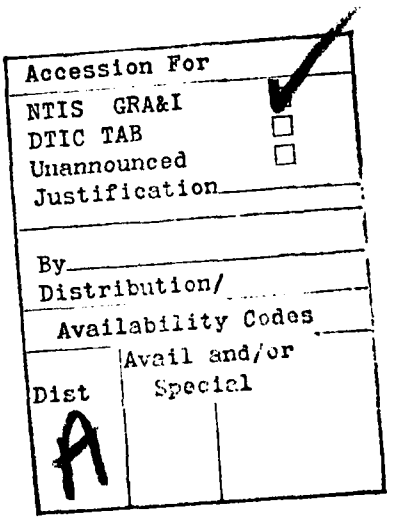

The responsibility for the wording and views expressed in this descriptive summary lies with MRC, and not with the author of this report.

SOLUTION OF PACKED-BED HEAT-EXCHANGER MODELS BY ORTHOGONAL COLLOCATION USING PIECEWISE CUBIC HERMITE FUNCTIONS

Anthony G. Dixon

Introduction

The choice of a model to describe heat transfer in packed beds is one which has often been dictated by the requirement that the resulting model equations should be relatively easy to solve for the bed temperature profile. This consideration has led to the widespread use of the pseudo-homogeneous two-dimensional model, in which the tubular bed is modelled as though it consisted of one phase only. This phase is assumed to move in plug-flow, with superimposed axial and radial effective thermal conductivities, which are usually taken to be independent of the axial and radial spatial coordinates. In non-adiabatic beds, heat transfer from the wall is governed by an apparent wall heat transfer coefficient.

The earliest heat-transfer studies neglected the effective axial conduction term as this was expected to be negligible by comparison with the bulk-flow term in the long beds typically used in industry. Axial dispersion was also neglected in mixing studies, and experiments by Hiby (1) confirmed the absence of axial back-mixing. Some studies have questioned this omission (2,3). More recently it has been shown (4,5) that measurements of temperature profiles in non-reacting systems in laboratory packed bed heat exchangers can yield statistically meaningful heat transfer parameter estimates only if the measurements are made at relatively short bed depths, where significant axial and radial temperature gradients are present. The omission of axial conduction at such bed depths leads to systematic errors in the predicted temperature profiles, which cause the model to be statistically rejected when it is fitted to data taken at several bed depths. If the model is fitted depth-by-depth, the parameter estimates are found to have a depth-dependence, as noticed by De Wasch and Froment (6). In this case, they must be regarded as length-

Sponsored by the United States Army under Contract No. DAAG29-80-C-0041 and the National Science Foundation under Grant No. ENG76-24368.

averaged values rather than point values. Li and Finlayson (7) argue that constant asymptotic values should be used, as obtained from data taken at long bed depths; this would give badly-determined estimates as noted above.

When a chemical reaction is present, implying larger temperature gradients, Young and Finlayson (8) have shown that an effective axial dispersion term should be included, and Mears (9) has given criteria for the neglect of axial dispersion which show that increasing fluid velocity reduces axial effects. This is to be expected, since conduction through the solid, a static effect, is believed to be the major contributor to axial effects.

The disadvantage of including axial dispersion is that an exit boundary condition must be specified, and in cases where an analytical solution is not available, a numerical boundary-value problem must be solved in the axial direction, rather than an initial-value problem. This point has been discussed recently by Jackson and co-workers (10), who present a cross-flow model of dispersion which allows downstream propagation but not upstream. However it would not be possible to use a one-phase model of this form for heat transfer, as axial back-conduction cannot be represented.

For steady-state heat transfer an elliptic partial differential equation is the result of using the one-phase model. Previous studies (8,11) have used the orthogonal collocation method due to Villadsen and Stewart (12) to determine the coefficients of trial-function expansions in both spatial co-ordinates. This method works well when the temperature gradients are moderate and few collocation points are required. For steep profiles, however, such as may be encountered at a "hot-spot" in the reactor, many collocation points may be required, especially as the generation of these points as roots of polynomials does not allow them to be placed in the region of interest. Such a collocation scheme is a global one, resulting in a collocation matrix which is large and not usefully sparse, so that the solution of the resulting algebraic equations may become costly. Furthermore, the polynomial collocation method has been known to oscillate about the true solution as the degree of approximation is increased (13).

The answer to these difficulties lies in the use of piecewise approximants, such as cubic splines, which are in general use in the mathematics literature (14). Carey and Finlayson (15) have introduced a finite-element collocation method along these lines, which uses polynomial approximants on sub-intervals of the domain, and apply continuity conditions at the break-points to smooth the solution. It would seem more straightforward, however, to use piecewise polynomials which do not require explicit continuity equations; in this paper the use of piecewise cubic Hermite functions is considered, as described by Prenter and Russell (16).

The advantages of piecewise polynomials are firstly that the subintervals may be clustered in regions of interest, so that an improved approximation may be obtained where gradients are steep, and secondly that the collocation matrix is banded, allowing advantage to be taken of this special structure, both in work required for decomposition and in computer storage used. This second advantage was clearly demonstrated in a preliminary study on the one-phase model (17), where the cubic Hermite function method was shown to give an order-of-magnitude improvement in exit temperature profile over the polynomial collocation method even when the subintervals were chosen to be of equal length. A more extensive investigation using the one-phase model as a test case is described in the present work.

The use of two-phase homogeneous continuum models in packed bed modelling has often been avoided due to the computational difficulties. Recently, Paspek and Varma (18) have found a two-phase model to be necessary to describe an adiabatic fixed-bed reactor, while Dixon and Cresswell (19) have shown that the effective parameters of the one-phase model may be interpreted in terms of the more fundamental parameters of a two-phase model, thus demonstrating more clearly their qualitative dependencies on the operating and design characteristics of the bed. When two phases and several species are involved, the computational advantages of the cubic Hermite method may be anticipated to be high.

In this paper the coupled elliptic partial differential equations arising from a two-phase homogeneous continuum model of heat transfer in a packed bed are solved, and some attempt is made to discriminate between rival correlations for those parameters not yet well-established, by means of a comparison with experimental results from a previous study (4,5).

Collocation using piecewise cubic Hermite functions

a) Boundary-value problems

The interval $[a,b]$ is partitioned into n subintervals by $a = \xi_1 < \xi_2 < \ldots < \xi_n < \xi_{n+1} = b$. Then the piecewise cubic Hermite functions are defined for $1 \le i \le n+1$ by

$$\phi_i(\xi) = \begin{cases} \dfrac{-2(\xi-\xi_{i-1})^3}{h_{i-1}^3} + \dfrac{3(\xi-\xi_{i-1})^2}{h_{i-1}^2} & (\xi_{i-1} \le \xi \le \xi_i) \\ 1 + \dfrac{2(\xi-\xi_i)^3}{h_i^3} - \dfrac{3(\xi-\xi_i)^2}{h_i^2} & (\xi_i \le \xi \le \xi_{i+1}) \\ 0 & \text{otherwise} \end{cases}$$

$$\psi_i(\xi) = \begin{cases} \dfrac{(\xi-\xi_{i-1})^2(\xi-\xi_i)}{h_{i-1}^2} & (\xi_{i-1} \le \xi \le \xi_i) \\ \dfrac{(\xi-\xi_i)(\xi_{i+1}-\xi)^2}{h_i^2} & (\xi_i \le \xi \le \xi_{i+1}) \\ 0 & \text{otherwise} \end{cases} .$$

The length of subinterval $[\xi_i,\xi_{i+1}]$ is denoted by h_i. The functions ϕ_1, ψ_1 are restricted to the interval $[\xi_1,\xi_2]$ and ϕ_{n+1}, ψ_{n+1} are restricted to the interval $[\xi_n,\xi_{n+1}]$.

The piecewise cubic Hermite interpolation polynomial to a function $u(\xi)$ is

$$u(\xi) \approx s_n(\xi) = \sum_{k=1}^{n+1} u(\xi_k)\phi_k(\xi) + u'(\xi_k)\psi_k(\xi) .$$

Hence $s_n(\xi)$ interpolates u and its first derivative u' at the points of the partition.

The Gaussian points of subinterval $[\xi_i, \xi_{i+1}]$ are $\xi_{i1} = \xi_i + (\sqrt{3} - 1)h_i/2\sqrt{3}$, $\xi_{i2} = \xi_{i+1} - (\sqrt{3} - 1)h_i/2\sqrt{3}$. Now define

$$\underline{u}_i = (u(\xi_i),\ u'(\xi_i),\ u(\xi_{i+1}),\ u'(\xi_{i+1}))$$

and, for $\xi_i \leq \xi \leq \xi_{i+1}$,

$$\underline{a}_i(\xi) = (\phi_i(\xi),\ \psi_i(\xi),\ \phi_{i+1}(\xi),\ \psi_{i+1}(\xi))$$

$$\underline{b}_i(\xi) = \frac{d}{d\xi}\,(\underline{a}_i(\xi))$$

$$\underline{c}_i(\xi) = \frac{d^2}{d\xi^2}\,(\underline{a}_i(\xi)) \quad .$$

Further, let $\underline{a}_i(\xi_{ij}) = \underline{a}_{ij}$ and similarly for $\underline{b}_{ij}$ and $\underline{c}_{ij}$.

Then

$$u(\xi_{ij}) \simeq s_n(\xi_{ij}) = (\underline{a}_{ij} \cdot \underline{u}_i)$$

$$u'(\xi_{ij}) \simeq s_n'(\xi_{ij}) = (\underline{b}_{ij} \cdot \underline{u}_i)$$

and

$$u''(\xi_{ij}) \simeq s_n''(\xi_{ij}) = (\underline{c}_{ij} \cdot \underline{u}_i) \quad .$$

The $2n+2$ unknown constants in $s_n(\xi)$ are determined by collocation at the $2n$ Gaussian points and use of the two boundary conditions. Computational details are given in the appendix, and an illustrative example is shown below.

Example: comparison of some collocation methods for a boundary-value problem.

The following problem is a good test case (27), giving a "boundary-layer" type of problem:

$$u''(x) + 2\gamma x u'(x) + 2\gamma u(x) = 0 \qquad (1)$$

$$u(0) = 1 \quad , \quad u(1) = e^{-\gamma} \quad . \qquad (1a,1b)$$

The solution is $u(x) = e^{-\gamma x^2}$, which falls steeply from $u = 1$ at $x = 0$ at a rate determined by the parameter γ.

The following methods are considered:

i) polynomial collocation, implemented using the routines given in (21).

ii) finite element collocation, implemented as described in (15).

iii) cubic Hermite collocation, as described above.

In case (i), collocation was performed at the zeros of $P_N^{(1,1)}(x)$, giving a system of N algebraic equations. For methods (ii) and (iii) the interval $[0,1]$ is divided into n subintervals by the set of breakpoints $\{x_i\}$. In the case of finite-element collocation it was found to be more effective to collocate at only two points per subinterval, and to increase the number of subintervals, rather than to increase the number of interior collocation points in each subinterval. Continuity equations must also be included for case (ii) at the breakpoints; this results in a system of size $3n + 1$, with a bandwidth of 7.

The equations for method (iii) in the above notation are

$$(\underline{c}_{ij} + 2\gamma x_{ij}\underline{b}_{ij} + 2\gamma \underline{a}_{ij}) \cdot \underline{u}_i = 0$$

$$j = 1,2 \quad ; \quad i = 1,2\ldots n$$

$$u(x_1) = 1 \quad ; \quad u(x_{n+1}) = e^{-\gamma} \quad .$$

These give a system of order $2n + 2$, with a bandwidth of 5. The same breakpoints were used for methods (ii) and (iii).

The difference between approximate and exact solutions was examined at the points $x = 0.01(0.01)0.10(0.10)0.90$; the maximum absolute error is denoted by $\|e\|_\infty$.

Some results are shown in tables 1 and 2. The times shown are relative and have no absolute meaning. Both methods (ii) and (iii) are seen to be faster for the same accuracy than method (i), especially for the case $\gamma = 1500$ which involves an extremely steep

gradient. Methods (ii) and (iii) gave the same results, as expected, with method (iii) being faster due to the fewer number of equations needed. The performance of methods (ii) and (iii) depended on the breakpoints used, a non-uniform mesh being the best choice. These were chosen heuristically, however it should be noted that simply aggregating points near $x = 0$ did not always give the best results.

Method (i)			Breakpoint set	$\|e\|_\infty$	Time	
N	$\|e\|_\infty$	Time			Method (ii)	Method (iii)
10	0.32	1.7	0(0.05)1.0	$0.30_{10}-2$	1.9	1.4
20	$0.52_{10}-3$	4.7	0(0.01)1.0	$0.32_{10}-5$	6.0	4.1
30	$0.39_{10}-5$	10.3				
40	$0.21_{10}-8$	19.4	0(0.005)0.1 (0.01)0.3(0.1) 1.0	$0.44_{10}-6$	3.4	2.5

Table 1 $\gamma = 150$

Method (i)			Breakpoint set	$\|e\|_\infty$	Time	
N	$\|e\|_\infty$	Time			Method (ii)	Method (iii)
10	0.22	1.7	0(0.001)0.05 (0.01)0.1(0.1) 1.0	$0.49_{10}-4$	4.3	3.0
20	0.12	4.7				
30	0.13	10.3				
40	$0.22_{10}-1$	19.5				
50	$0.59_{10}-3$	32.4	0(0.001)0.1 (0.05)1.0	$0.95_{10}-7$	7.0	4.8

Table 2 $\gamma = 1500$

b) Elliptic partial differential equations

The use of piecewise bicubic Hermite functions in collocation schemes for the solution of elliptic partial differential equations has been described by Prenter (16,20); a short outline is presented here.

Partition the domain $[a,b] \times [c,d]$ by

$$a = y_1 < y_2 < \ldots < y_n < y_{n+1} = b$$

and

$$c = x_1 < x_2 < \ldots < x_m < x_{m+1} = d$$

then the piecewise bicubic Hermite interpolation polynomial to a function $\theta(y,x)$ is

$$\theta(y,x) \simeq s_{n,m}(y,x)$$

$$= \sum_{i=1}^{n+1} \sum_{j=1}^{m+1} \{\theta(y_i,x_j)\phi_i(y)\phi_j(x) + \frac{\partial\theta}{\partial y}(y_i,x_j)\psi_i(y)\phi_j(x)$$

$$+ \frac{\partial\theta}{\partial x}(y_i,x_j)\phi_i(y)\psi_j(x) + \frac{\partial^2\theta}{\partial y\partial x}(y_i,x_j)\psi_i(y)\psi_j(x)\} \quad .$$

This involves $4(n+1)(m+1)$ unknown constants. The Gaussian points for the x and y directions are defined as before; combining the two points for each of $[y_i,y_{i+1}]$ and $[x_j,x_{j+1}]$ gives four Gaussian points for the subrectangle $[y_i,y_{i+1}] \times [x_j,x_{j+1}]$. Collocation at these points for each subrectangle yields a total of $4nm$ equations. It should be noted that at any collocation point $(y_{ik},x_{j\ell})$ only sixteen bicubic product functions are non-zero, hence each collocation equation involves only sixteen unknowns.

Now let $\underline{\theta}_{ij} = (\theta(y_i,x_j), \frac{\partial\theta}{\partial y}(y_i,x_j), \frac{\partial\theta}{\partial x}(y_i,x_j), \frac{\partial^2\theta}{\partial y\partial x}(y_i,x_j))$ and

$$\underline{\theta} = (\underline{\theta}_{ij}, \underline{\theta}_{i+1,j}, \underline{\theta}_{i,j+1}, \underline{\theta}_{i+1,j+1})^t \quad .$$

Let $\underline{a}_{ij}(y,x) = (\phi_i(y)\phi_j(x), \psi_i(y)\phi_j(x), \phi_i(y)\psi_j(x), \psi_i(y)\psi_j(x))$ and

$$\underline{A}_{ij}(y,x) = (\underline{a}_{ij}(y,x),\ \underline{a}_{i+1,j}(y,x),\ \underline{a}_{i,j+1}(y,x),\ \underline{a}_{i+1,j+1}(y,x))$$

then

$$\underline{B}^{x}_{ij}(y,x) = \frac{\partial}{\partial x}(\underline{A}_{ij}(y,x))$$

$$\underline{B}^{y}_{ij}(y,x) = \frac{\partial}{\partial y}(\underline{A}_{ij}(y,x))$$

$$\underline{C}^{xx}_{ij}(y,x) = \frac{\partial^2}{\partial x^2}(\underline{A}_{ij}(y,x))$$

$$\underline{C}^{yy}_{ij}(y,x) = \frac{\partial^2}{\partial y^2}(\underline{A}_{ij}(y,x))$$

$$\underline{C}^{yx}_{ij}(y,x) = \frac{\partial^2}{\partial y \partial x}(\underline{A}_{ij}(y,x)) \quad .$$

In particular, $\underline{A}_{ij}(y_{ik},x_{j\ell}) = \underline{A}_{ijk\ell}$ and similarly for the others.

Then $\phi(y_{ik},x_{j\ell}) = (\underline{A}_{ijk\ell} \cdot \underline{\phi}_{ij})$ and again similar expressions hold for derivatives of ϕ.

The above provides a concise notation for the collocation equations.

The remaining $4n + 4m + 4$ equations required to determine the expansion coefficients are supplied by the boundary conditions as follows:

(i) on the lines $y = 0$ and $y = 1$, the boundary conditions given are differentiated with respect to x. Together with the original equations this yields two equations on each boundary, which may be applied at each of the $m - 1$ internal boundary nodes to obtain a total of $4m - 4$ conditions. For example, given $\frac{\partial \phi}{\partial y} = 0$ at $y = 0$, then $\frac{\partial^2 \phi}{\partial y \partial x} = 0$ at $y = 0$ also, and hence

$$\left.\begin{aligned} \frac{\partial \phi}{\partial y}\ (0,x_i) &= 0 \\ \frac{\partial^2 \phi}{\partial y \partial x}\ (0,x_i) &= 0 \end{aligned}\right\} \quad i = 2,3\ldots m$$

(ii) a similar procedure may be followed on the lines $x = 0$, $x = 1$, to obtain $4n - 4$ conditions.

(iii) at each corner both (i) and (ii) above may be applied, to give four conditions. However only three of these will be independent, and one must be eliminated, except when there is a corner discontinuity, when an arbitrary decision must be made.

The $4n + 4m + 4$ conditions derived above may be used either to eliminate unknowns and thus reduce the size of the system of equations to be solved, as was done in the original paper (16), or to generate extra equations. The latter procedure is easier to apply when mixed boundary conditions are used, the resulting increase in computer time used being offset by the saving in programming effort.

c) Parabolic partial differential equations

The solution of parabolic partial differential equations by the cubic Hermite function method and by several other methods has been reviewed by Hopkins and Wait (23). They also provide extensive program listings for the solution of the set of ODEs which results.

One-phase continuum model

The packed bed heat exchanger considered here is that used in recent experimental studies (3,5) and shown schematically in figure 1. The long unheated calming section, (a), and the heated test section, (b), are each considered to be semi-infinite and packed with similar solid particles. There is a step change in wall temperature at the plane $z = 0$.

The model equations are well-known, and are, in dimensionless form,

$$\frac{\partial\theta}{\partial x} = \frac{1}{Pe_A}\frac{\partial^2\theta}{\partial x^2} + \frac{1}{Pe_R}\left(\frac{\partial^2\theta}{\partial y^2} + \frac{1}{y}\frac{\partial\theta}{\partial y}\right) \tag{2}$$

$$\frac{\partial\theta}{\partial y} = 0 \quad \text{at} \quad y = 0 \tag{3}$$

$$\theta \to 0 \quad \text{as} \quad x \to -\infty \tag{4}$$

$$\theta \to 1 \quad \text{as} \quad x \to \infty \tag{5}$$

$$\frac{\partial\theta}{\partial y} + (Bi)\theta = (Bi)H(x) \quad \text{at} \quad y = 1 \tag{6}$$

Here the Heaviside step function is used to model the change in wall temperature. The downstream axial boundary condition, equation 5, was found to be consistent with experimental data in a previous study (5).

The equations (2) - (6) have an easily-determined analytic series solution in terms of Bessel functions (5); this is therefore a good test case upon which to try out the numerical method.

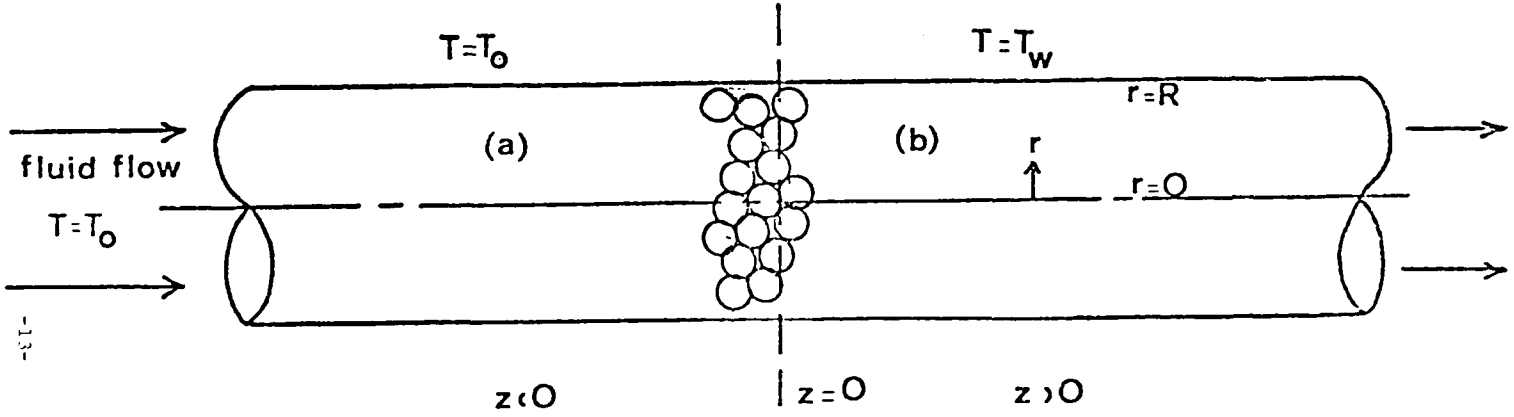

FIG. 1: SCHEMATIC REPRESENTATION OF PACKED BED

There are two points of interest associated with the numerical solution of equations (2) - (6): (i) the x-domain is infinite and (ii) there is a step-function in the wall boundary condition.

(i) Transformation of the infinite domain

There are several ways of dealing with an infinite domain. Guertin et al (24) chose perturbation solutions of the model as basis functions. This approach may be difficult to extend to more complicated equations than the non-linear initial-value problems which they considered; even so, the modeller must do a considerable amount of analytical work with this method.

Birnbaum and Lapidus (25) suggest the use of polynomials which are orthogonal over the infinite domain, obtaining these either by using a weighting function such as e^{-x^2}, which gives Hermite polynomials orthogonal over $(-\infty,\infty)$, or by transforming the infinite domain onto a finite domain, and using conventional polynomials such as shifted Legendre polynomials. The drawback to these methods is that there is no control of the placement of the collocation points, some of which are always included in regions where the profile is essentially flat, and are thus wasted.

The use of standard piecewise polynomials, together with an appropriate transformation of the infinite domain, overcomes these difficulties, provided some care is taken in the transformation.

Verhoff and Fisher (26) used the form $t = \frac{1}{\pi}\tan^{-1}(\frac{x}{\alpha})$ in their solution of the Graetz problem with axial conduction. Somewhat neater equations result from taking $t = \tanh(x/\alpha)$ giving

$$(\frac{1-t^2}{\alpha})(1 + \frac{2t}{\alpha Pe_A})\frac{\partial\theta}{\partial t} = \frac{1}{Pe_P}(\frac{\partial^2\theta}{\partial y^2} + \frac{1}{y}\frac{\partial\theta}{\partial y}) + \frac{(1-t^2)^2}{\alpha^2 Pe_A}\frac{\partial^2\theta}{\partial t^2} \qquad (7)$$

$$\frac{\partial\theta}{\partial y} = 0 \quad \text{at} \quad y = 0 \qquad (8)$$

$$\theta = 0 \quad \text{at} \quad t = -1 \qquad (9)$$

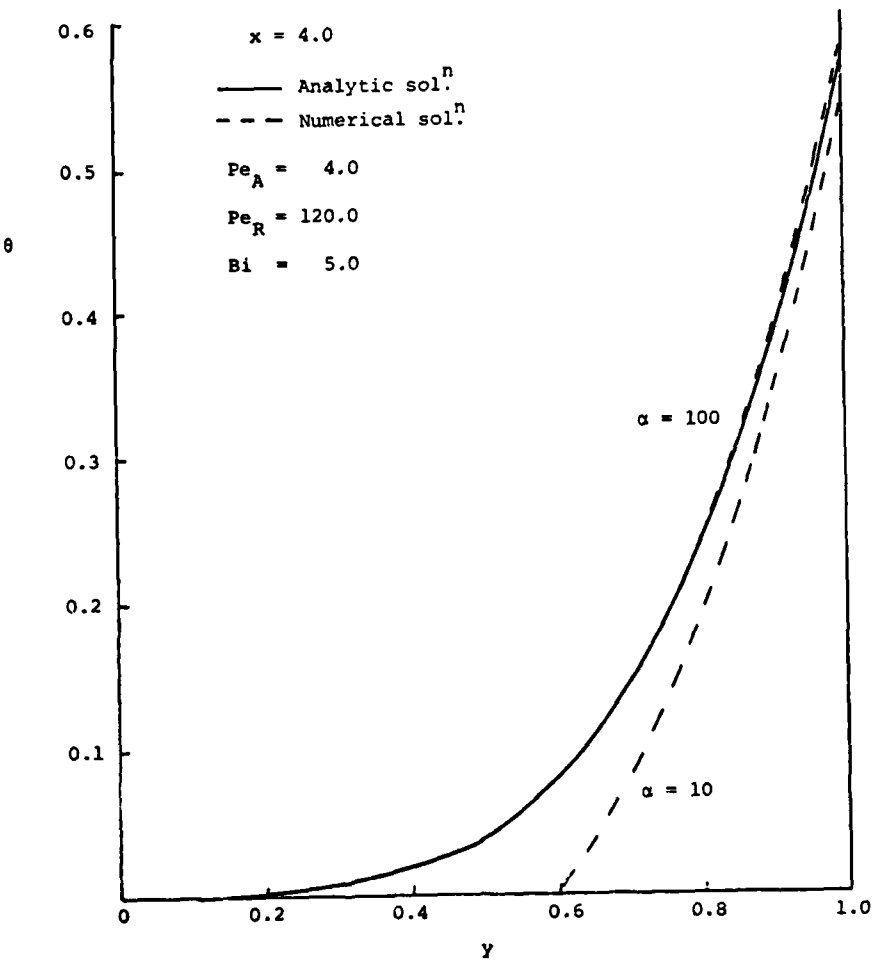

FIG. 2: EFFECT OF CHOICE OF SCALING FACTOR α

The collocation equations for this case are:

$$\left(\frac{(1 - t_{jv}^2)}{\alpha}\left(1 + \frac{2t_{jv}}{\alpha Pe_A}\right)\underline{B}^{t}_{ijuv} - \frac{(1 - t_{jv}^2)^2}{\alpha^2 Pe_A}\underline{C}^{tt}_{ijuv}\right.$$

$$\left. - \frac{1}{Pe_F}\left(\underline{C}^{yy}_{ijuv} + \frac{1}{y_{iu}}\underline{B}^{y}_{ijuv}\right)\right).\ \underline{\phi}_{ij} = 0$$

$$u = 1,2 \ ; \ v = 1,2 \ ; \ i = 1,2...,n \ ; \ j = 1,2...,m \ .$$

Here $\underline{\phi}_{ij}$ is the vector of unknowns for subrectangle ij.

The boundary conditions are:

$$\frac{\partial\theta}{\partial y}(0,t_j) = 0 \qquad (j = 2,3...m)$$

$$\frac{\partial^2\theta}{\partial y \partial t}(0,t_1) = 0 \qquad (j = 1,2...m+1)$$

$$\theta(y_i, -1) = \frac{\partial\theta}{\partial y}(y_i, -1) = 0 \qquad (i = 1,2...n+1)$$

$$\left.\begin{aligned}\theta(y_i, 1) &= 1.0 \\ \frac{\partial\theta}{\partial y}(y_i, 1) &= 0\end{aligned}\right\} \qquad (i = 1,2...n+1)$$

$$\left(\underline{B}^{y}_{nj}(1, t_{jk}) + (Pi)\ \underline{A}_{nj}(1, t_{jk})\right).\ \underline{\phi}_{nj} = (Pi)\ H(t_{jk})$$

$$k = 1,2 \ , \ j = 1,2...m \ .$$

The natural ordering of equations (16) gives a bandwidth of $4n + 15$.

When considering the degree of accuracy to be required from a numerical method, it is necessary to take into account the potential uses of the model equations being solved. It would be inappropriate to require high accuracy in the present study, as bed temperature profiles are seldom accurately measured. Consequently errors of 1°C in comparing numerical and analytical results were considered reasonable.

$$\theta = 1 \quad \text{at} \quad t = 1 \tag{10}$$

$$\frac{\partial \theta}{\partial y} + (Bi)\theta = Pi\ H(t) \tag{11}$$

Initially it may appear simplest to let $\alpha = 1$, and use $t = \tanh x$. However this results in the region $x > 3$ in the bed being mapped onto a small interval [0.995,1]. This is undesirable for two reasons:

1) If subintervals are required in the bed downstream of $x = 3$, it becomes difficult to place the breakpoints in the t-domain

2) if axial gradients are present downstream of $x = 3$, they will become very sharp in the t-domain, since $\frac{\partial \theta}{\partial t} = \frac{\alpha}{(1-t^2)} \frac{\partial \theta}{\partial x}$ so $\frac{\partial \theta}{\partial t} \to \infty$ as $t \to 1$.

It can be seen that for a fixed choice of $\{t_i\}$, different choices of α will locate the induced partition $\{x_i\}$ in different physical parts of the bed. Thus α must be chosen so that the collocation points in the t-domain are placed in a way that makes physical sense in the x-domain. The appropriate value is found by trial and error; an empirical rule suggested by experience is to take $\alpha = Pe_R$.

The effect of an inappropriate value for α is shown in figure 2. It should be noted that although Verhoff and Fisher used $\alpha = 1$ throughout, their computations were made for sufficiently short beds to ensure good results; larger values of α would be required for temperature profiles further downstream, which would be of interest in the presence of reaction.

(ii) Step-change in wall boundary condition

It was anticipated that the discontinuity in wall temperature at $x = 0$, and the resulting steep local gradients, would lead to a locally poor approximation which might have adverse effects further downstream. It was soon found that mesh refinement in the axial direction improved the results considerably over the use of an equally-spaced mesh, whereas mesh refinement in the radial direction had little effect, and a fairly coarse uniform radial mesh was always found to be adequate.

The mesh refinement was carried out by heuristically searching for good breakpoint distributions, the final choice (corresponding to $m = 10$) being

$$\{t_j\} = \{-0.1, -0.05, -0.025, 0, 0.025, 0.05, 0.1, 0.2, 0.6\} \quad .$$

Any further refinement led to improved values only at extremely short bed depths.

The effect of the wall temperature discontinuity may also be mitigated by an alternative implementation of the wall boundary condition to that described in the previous section. The two equations at each interior boundary node $(1,t_j)$, $j = 2,3,\ldots,m$, are dropped, together with one equation at each of $(1,-1)$ and $(1,1)$. These $2m$ equations are replaced by application of the boundary conditions at two points within each subinterval on the line $y = 1$. The Gaussian points are not necessarily the optimal choice, but were used in the absence of any other guideline.

For the case of a uniform mesh, the Gaussian point implementation was an order-of-magnitude improvement over the breakpoint implementation. When the refined mesh was used, the two methods gave essentially the same results, except at low bed depths near the wall, where the Gaussian point method was slightly better. Consequently it was the method used in the rest of the work.

The reason for the above differences is not clear but appears to lie in the wall temperature specification. No difference between the methods was found when applied to the centre-line condition, and reduction of Bi to lessen effects of the discontinuity also greatly reduced the advantage of the Gaussian point method. It may be that the boundary condition is more effective when "spread out" using two points instead of being reinforced by applying two conditions at one point.

The comparisons were made at $y = 0.1,0.2...1.0$ for each of 5 bed depths: $x = 1.33,2.67,4.00,5.33,6.67$. The parameter ranges covered were

$$Pe_A : 0.25 - 20.0$$

$$Pe_R : 2.5 - 120.0$$

$$Bi : 0.5 - 8.0 .$$

The refined mesh given above was used in the axial direction; the radial mesh used $n = 3$, $\{y_i\} = \{0.25,0.5,0.75\}$. It was found possible to use the same mesh throughout in the t-domain, due to the freedom to vary the scaling factor α. This avoided heuristic searching for a new mesh for each new set of parameters. Automatic mesh generation was not felt to be worthwhile, in view of the extra costs involved and the relatively underdeveloped state of the art (27).

The 1°C criterion was met in all cases except for $Pe_A = 20$ using this method. For that case the centre-line discrepancy rose to approximately 3°C at lower bed depths. Presumably this error could be eliminated by taking higher order approximations. Typical computation times to produce one set of solutions (i.e., 5 bed depths) were approximately 1.5 sec on a UNIVAC 1110 computer, a reasonable compromise between cost and accuracy.

Two-phase continuum model

Two-phase continuum models, in which the solid particles and their associated stagnant fillets of fluid are regarded as a continuous pseudo-solid phase, are to be preferred to the more traditional cell model of a particle bathed in fluid, which does not allow conduction from particle to particle. In previous studies, such models have been simplified by considering a one-dimensional model only (28). This study considers the full equations, which are, in dimensionless form:

$$\frac{1}{Pe_{RF}}\left(\frac{\partial^2 T_f}{\partial y^2}+\frac{1}{y}\frac{\partial T_f}{\partial y}\right)+\frac{1}{Pe_{AF}}\frac{\partial^2 T_f}{\partial x^2}-\frac{N_f}{Pe_{RF}}(T_f-T_s)=\frac{\partial T_f}{\partial x} \tag{12}$$

$$\left(\frac{\partial^2 T_s}{\partial y^2}+\frac{1}{y}\frac{\partial T_s}{\partial y}\right)+\frac{\partial^2 T_s}{\partial x^2}+N_s(T_f-T_s)=0 \tag{13}$$

$$\frac{\partial T_f}{\partial y}=\frac{\partial T_s}{\partial y}=0 \quad \text{at} \quad y=0 \tag{14}$$

$$\begin{aligned}\frac{\partial T_f}{\partial y}+(Bi_f)T_f&=(Bi_f)H(x)\\ \frac{\partial T_s}{\partial y}+(Bi_s)T_s&=(Bi_s)H(x)\end{aligned} \quad \text{at} \quad y=1 \tag{15}$$

$$T_f, T_s \to 0 \quad \text{as} \quad x \to -\infty \tag{16}$$

$$T_f, T_s \to 1 \quad \text{as} \quad x \to \infty \ . \tag{17}$$

A semi-analytical solution to these equations was derived by Dixon and Cresswell (19), who then matched the fluid phase temperature profile to the one-phase model profile to obtain explicit relations between the parameters of the two models.

The numerical solution to the system of equations (12) - (17) parallels that of the one-phase model almost exactly, with longer computation times due to the increased size of the collocation matrix and its bandwidth. Typical computation times to produce fluid and solid temperature profiles at each of five bed-depths were 3 - 4 seconds.

A discussion of the correlations available for prediction of the parameters required in the two-phase model is presented in (19); those chosen in this study were

$$\frac{1}{Pe_{RF}} = \frac{2d_p}{d_t}\left(\frac{1}{Pe_{rf}(\infty)} + \frac{0.67\varepsilon}{(Re)(Pr)}\right) \tag{18}$$

$$\frac{1}{Pe_{AF}} = \frac{2d_p}{d_t}\left(\frac{1/Pe_{af}(\infty)}{1.0 + 9.7\varepsilon/(RePr)} + \frac{0.73\varepsilon}{(RePr)}\right) \tag{19}$$

$$Bi_f = 0.12\ Pe_{rf}(\infty)\ \frac{d_t}{d_p}\ (Pr)^{-0.67}(Re)^{-0.25} \tag{20}$$

$$N_s = \frac{1.5(1-\varepsilon)(d_t/d_p)^2}{(k_{rs}/k_g)(1/Nu_{fs} + 0.1k_g/k_p)} \tag{21}$$

$$N_f = \frac{2d_p}{d_t}\left(\frac{k_{rs}}{k_g}\right)\frac{N_s Pe_{RF}}{(RePr)} \tag{22}$$

$$Nu_{fs} = \frac{0.255}{\varepsilon}\ (Pr)^{0.33}(Re)^{0.665} \quad . \tag{23}$$

As the fluid was air, Pr = 0.72; the bed voidage ε was taken as 0.4. The ratios k_{rs}/k_g and k_p/k_g were related using the formula of Zehner and Schlünder (30). Preliminary sensitivity tests showed that the parameter Nu_{fs} had very little effect on the profiles; in the presence of reaction this parameter would be more important.

It is clear that by adjusting the parameters of this model by nonlinear regression, an excellent fit to the experimental data could be obtained. The value of such a procedure is rather dubious, however, and it is more useful to use the model to obtain qualitative information about the quantities $Pe_{rf}(\infty)$, $Pe_{af}(\infty)$ and Bi_s, which are poorly determined in the literature.

a) $Pe_{rf}(\infty)$

This quantity is almost certainly a weak function of the tube-to-particle diameter ratio (d_t/d_p), although the exact dependence is not well-established. Examination of reported literature data, especially the results of Kunii et al (31) at extremely high Re, suggests taking $Pe_{rf}(\infty) = 8.0$.

b) $Pe_{af}(\infty)$

Recent work of Hsiang and Haynes (32) shows the commonly-taken value of $Pe_{af}(\infty) = 2.0$ to be questionable in the (d_t/d_p) range considered here. It was decided to use the relationship $Pe_{af} \simeq Pe_a$, which results from the model matching of (19) when $Re > 20$-30. The values of Pe_a were poorly determined from measurements made at bed exit alone (5), so estimates from data which included profiles at $z = 0$ were used (4). These values led to great improvements in the slopes of the predicted profiles.

c) Bi_s

Values of Bi_s may lie between the theoretical lower bound derived by Olbrich (29):

$$Bi_s > (2.12)\left(\frac{R}{d_p}\right)$$

and $Bi_s = \infty$, corresponding to no thermal resistance between solid and wall.

If equation (20) is used to predict Bi_e, then it is necessary to take $Bi_s = 1000$ for a good fit, as shown in figure 3 for a typical case. However, it should be noted that equation (20) underestimates the values of $Bi_e (= Bi)$ found in (5). This is probably due to the unreliable correlation used for Nu_{wf}, as pointed out in (4). If the experimental estimates of Bi are used instead of equation (20), then values of Bi_s in the range 10 - 20 are needed. Some of these results are shown in figures 6 - 7.

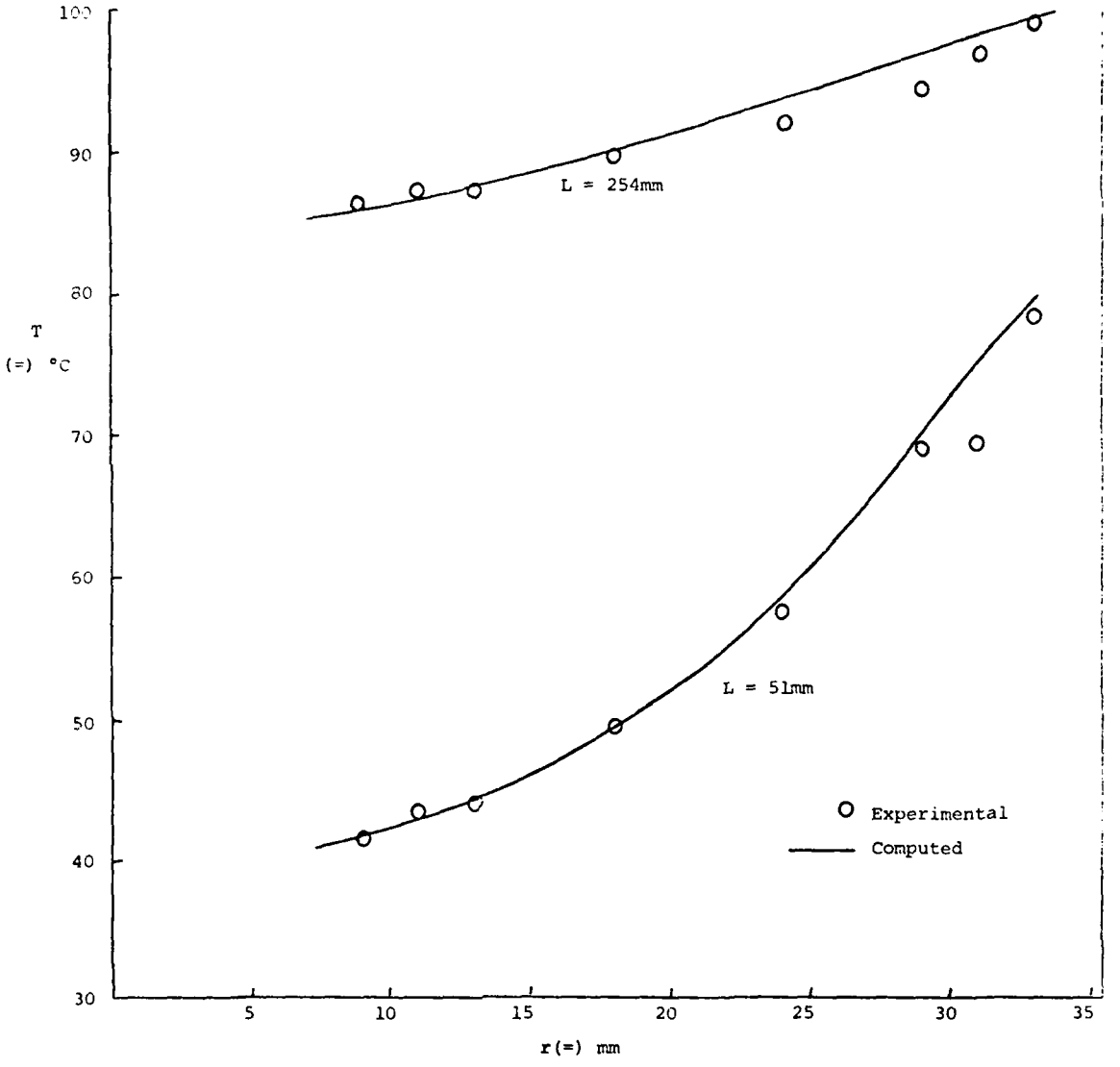

FIG. 3: 9.5mm CERAMIC BEADS

Re = 120

$Pe_{rf}(\infty)$ = 8.0 Bi_f = 3.35

$Pe_{af}(\infty)$ = 0.49 Bi_s = 1000

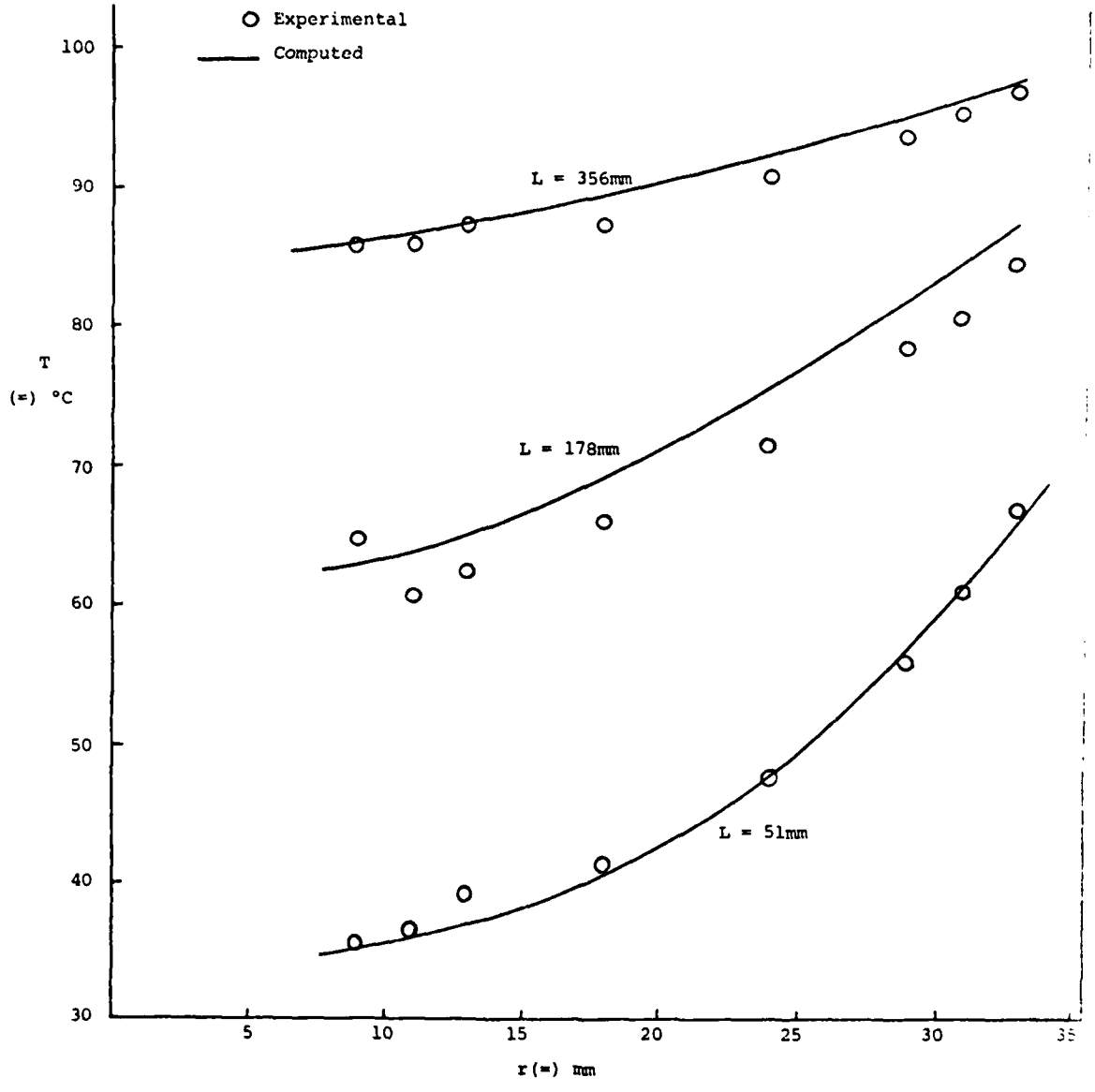

FIG. 4: 12.7mm CERAMIC BEADS

Re = 430

$Pe_{rf}(\infty)$ = 8.0 $\quad Bi_f$ = 2.85

$Pe_{af}(\infty)$ = 0.45 $\quad Bi_s$ = 10.0

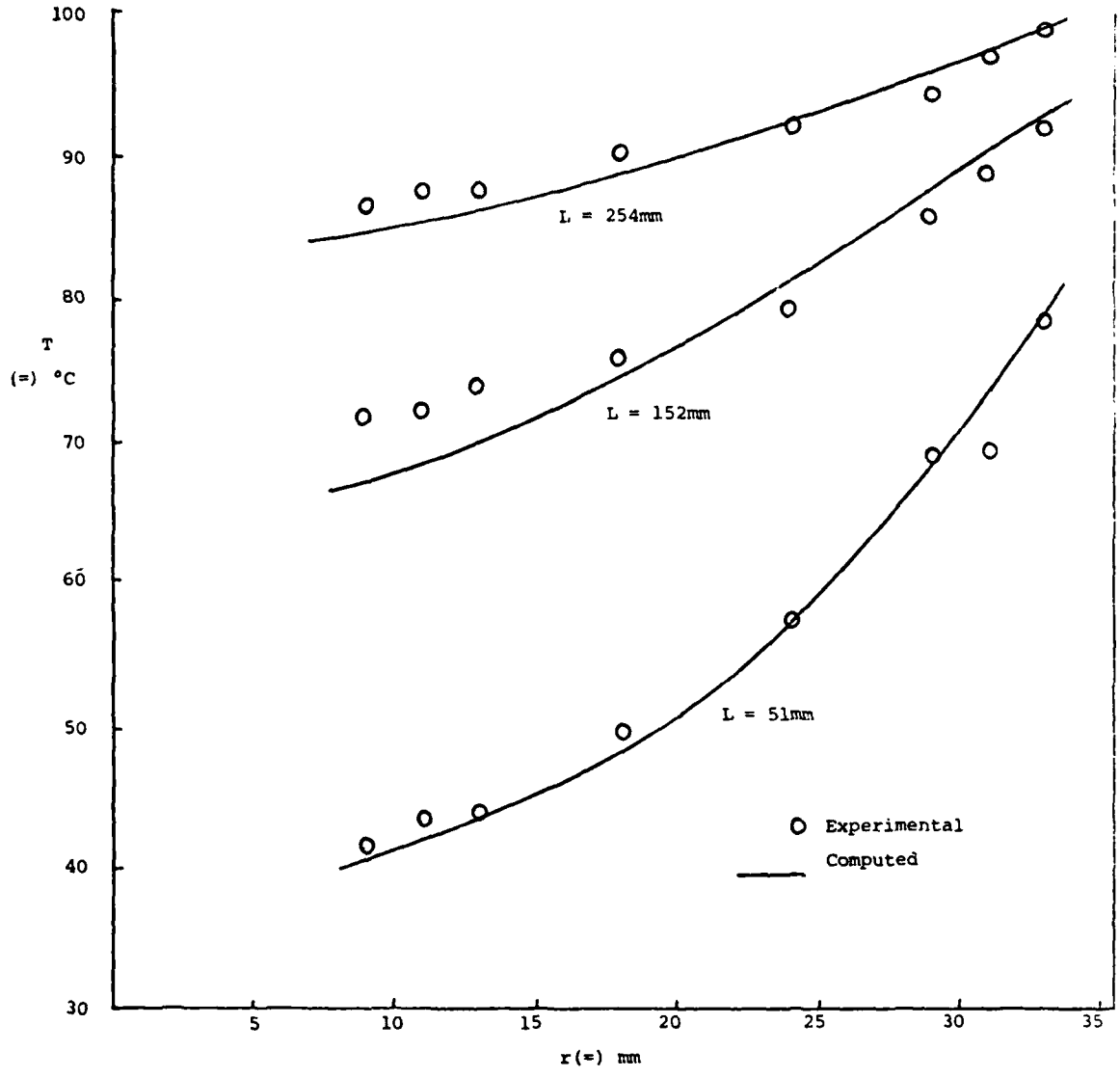

FIG. 5: 9.5mm CERAMIC BEADS

Re = 120

$Pe_{rf}(\infty)$ = 8.0 Bi_f = 4.57

$Pe_{af}(\infty)$ = 0.49 Bi_s = 20.0

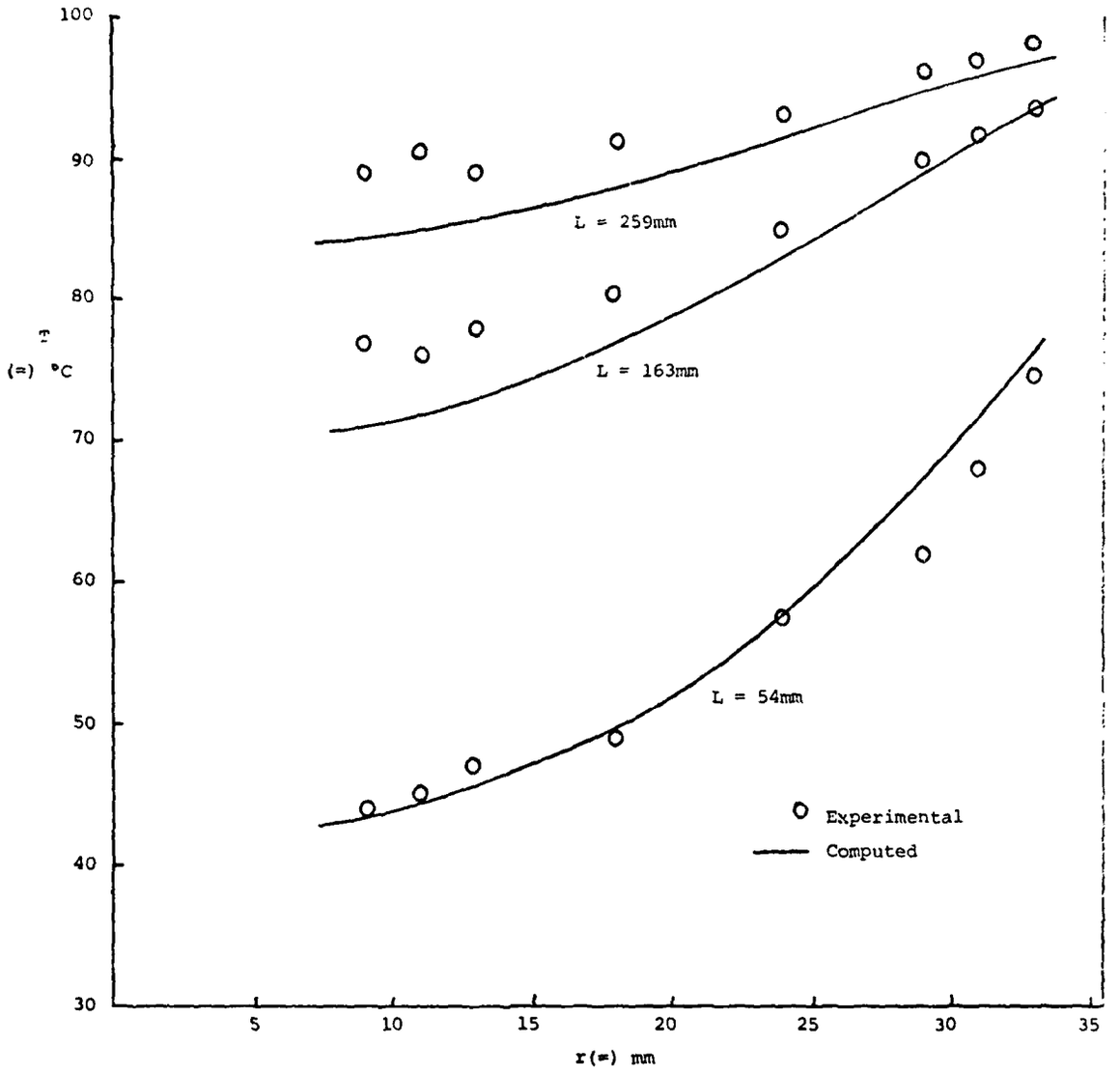

FIG. 6: 9.5mm STEEL BALLS

Re = 224

$Pe_{rf}(\infty)$ = 8.0 Bi_f = 3.9

$Pe_{af}(\infty)$ = 0.31 Bi_s = 20.0

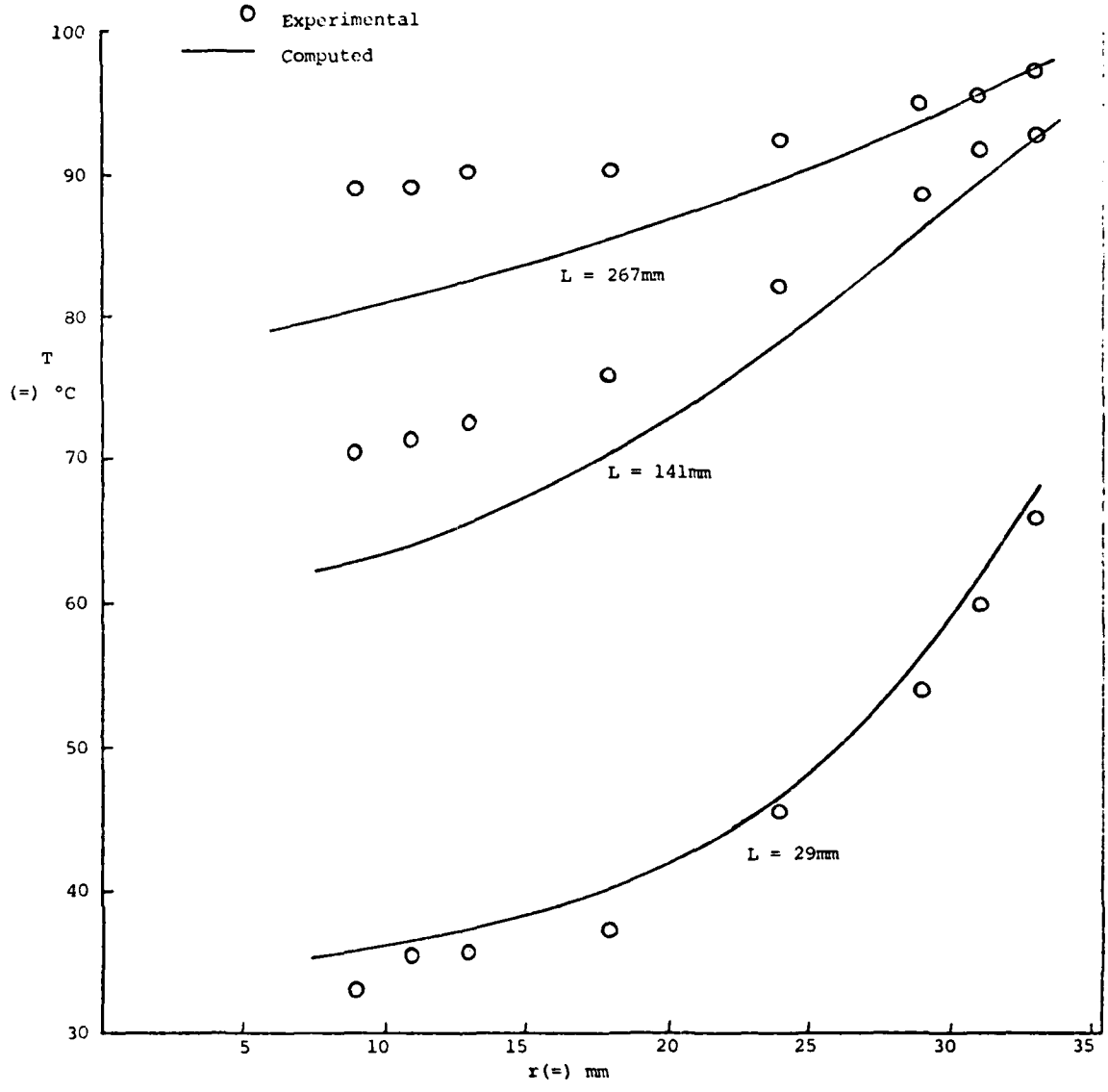

FIG. 7: 6.4mm CERAMIC BEADS

Re = 73

$Pe_{rf}(\infty)$ = 8.0 Bi_f = 5.85

$Pe_{af}(\infty)$ = 0.14 Bi_s = 20.0

This result indicates that only precise determination of Bi_f will allow any conclusions to be drawn on Bi_s, since these parameters may be mutually varied over fairly large ranges and similar results obtained.

The computed temperature profiles in figures 4 - 7 show good general agreement with experiment; some deviation is apparent in the centre of the bed for $Re = 73$ and 224. Agreement is improved if lower values of $Pe_{rf}(\infty)$ are used, but there is no justification for this in the literature.

The semi-analytical solution given in (19) may also be compared to experimental results using the same parameter results as for the numerical method. This is shown in figure 8 for the case $Re = 430$. Similar results to the numerical method are obtained at longer bed depths; at short bed depths the approximation is poor, due mainly to the inadequacy of the one-point radial collocation method used.

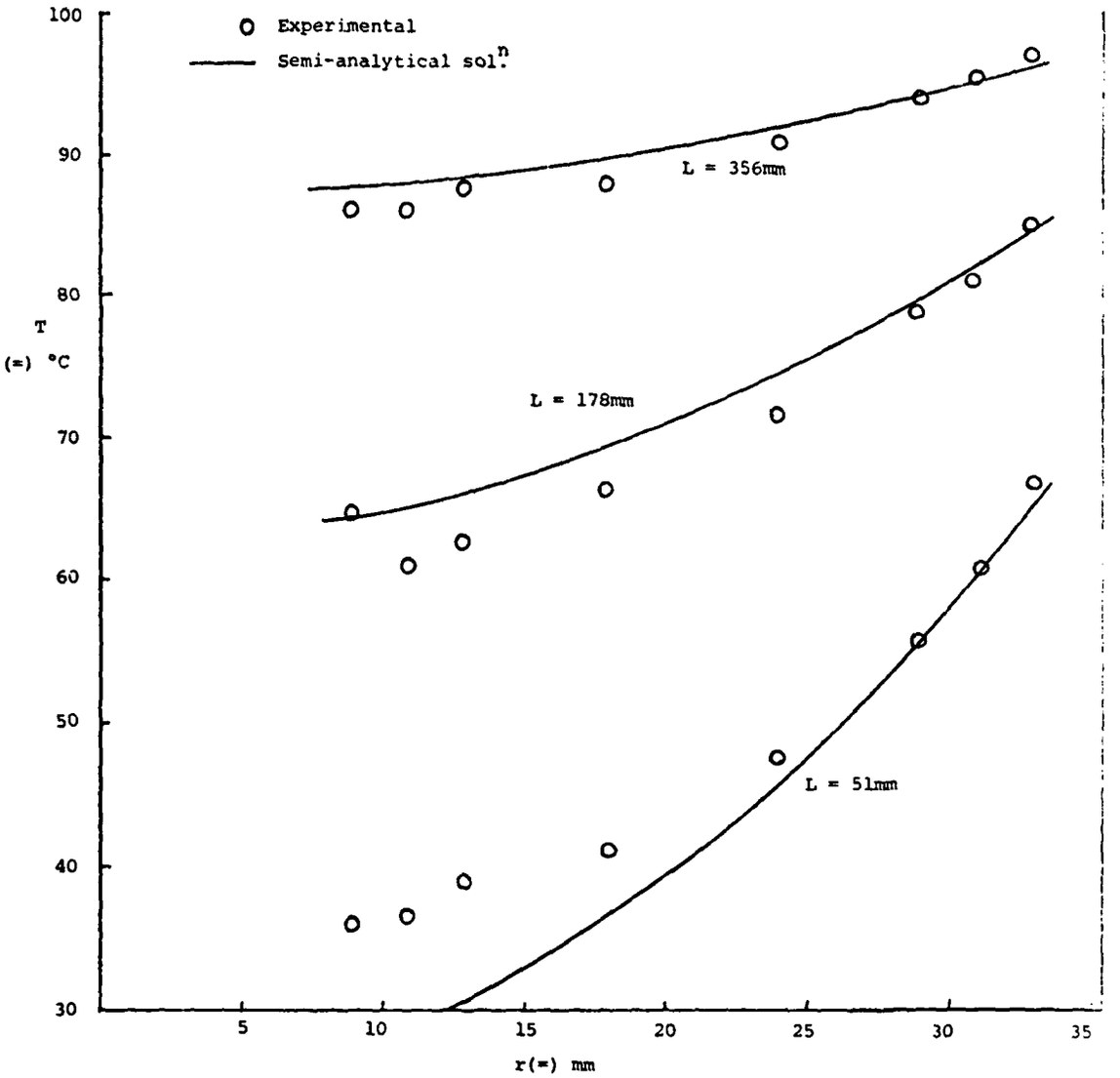

FIG. 8: 12.7mm CERAMIC BEADS

Re = 430

$Pe_{rf}(\infty)$ = 8.0 Bi_f = 2.85

$Pe_{af}(\infty)$ = 0.45 Bi_s = 10.0

Conclusions

The orthogonal collocation method using piecewise cubic Hermite polynomials has been shown to give reasonably accurate solutions at low computing cost to the elliptic partial differential equations resulting from the inclusion of axial conduction in models of heat transfer in packed beds. The method promises to be effective in solving the nonlinear equations arising when chemical reactions are considered, because it allows collocation points to be concentrated where they are most effective.

The fluid-phase temperatures predicted from a two-phase pseudo-homogeneous model were shown to give reasonable agreement with experimental measurements, without explicitly adjusting the model parameters. It was demonstrated that more refined experimental measurements will be needed to determine the parameters of the model; in particular, the solid and fluid phase wall Biot numbers were mutually adjustable.

NOMENCLATURE

a	specific interfacial surface area (m^{-1})
c_p	fluid specific heat (kJ/kg°C)
d_p	pellet diameter (m)
d_t	tube diameter (m)
G	superficial mass flow rate (kg/m^2s)
h	apparent interphase heat transfer coefficient ($w/m^{2\circ}C$)
h_w	apparent wall heat transfer coefficient ($w/m^{2\circ}C$)
h_{wf}	wall-fluid heat transfer coefficient ($w/m^{2\circ}C$)
h_{ws}	wall-solid heat transfer coefficient ($w/m^{2\circ}C$)
h_{fs}	fluid-solid heat transfer coefficient ($w/m^{2\circ}C$)
k_a	axial effective conductivity ($w/m^{\circ}C$)
k_r	radial effective conductivity ($w/m^{\circ}C$)
k_{af}	axial conductivity of fluid phase ($w/m^{\circ}C$)
k_{as}	axial conductivity of solid phase ($w/m^{\circ}C$)
k_{rf}	radial conductivity of fluid phase ($w/m^{\circ}C$)
k_{rs}	radial conductivity of solid phase ($w/m^{\circ}C$)
k_g	molecular conductivity of fluid ($w/m^{\circ}C$)
k_p	pellet conductivity ($w/m^{\circ}C$)
L	length of packed test section (m)
R	tube radius (m)
r	radial coordinate (m)
T_b	bed temperature, one-phase model (°C)
T_{bf}	fluid phase temperature (°C)
T_{bs}	solid phase temperature (°C)
T_0	temperature of calming section wall (°C)
T_w	temperature of test section wall (°C)
u	superficial fluid velocity (m/s)
z	axial co-ordinate (m)

Dimensionless parameters

Bi	apparent wall Biot number, h_wR/k_r
Bi_f	fluid-wall Biot number, $h_{wf}R/k_{rf}$
Bi_s	solid-wall Biot number, $h_{ws}R/k_{rs}$
h_i	subinterval length
m	number of axial subintervals

n	number of radial subintervals
N_F	interphase heat transfer group, aR^2h/k_{rf}
N_S	interphase heat transfer group, aR^2h/k_{rs}
Nu_w	apparent wall Nusselt number, $h_w d_p/k_g$
Nu_{fs}	fluid-solid Nusselt number, $h_{fs}d_p/k_g$
Nu_{wf}	fluid-wall Nusselt number, $h_{wf}d_p/k_g$
Pe_a	effective axial Peclet number, $Gc_p d_p/k_a$
Pe_A	effective axial Peclet number (based on R), Gc_pR/k_a
Pe_r	effective radial Peclet number, $Gc_p d_p/k_r$
Pe_R	effective radial Peclet number (based on R), Gc_pR/k_r
Pe_{af}	axial fluid Peclet number, $Gc_p d_p/k_{af}$
Pe_{AF}	axial fluid Peclet number (based on R), Gc_pR/k_{af}
Pe_{rf}	radial fluid Peclet number, $Gc_p d_p/k_{rf}$
Pe_{RF}	radial fluid Peclet number (based on R), Gc_pR/k_{rf}
$Pe_{rf}(\infty)$	asymptotic value of Pe_{rf} as $Re \to \infty$
$Pe_{af}(\infty)$	asymptotic value of Pe_{af} as $Re \to \infty$
Pr	Prandtl number, $\mu c_p/k_g$
Re	Reynolds number, Gd_p/μ
y	normalised radial co-ordinate (r/R)
t	transformed axial co-ordinate
T_f	dimensionless fluid temperature $(T_{bf}-T_0)/(T_w-T_0)$
T_s	dimensionless solid temperature $(T_{bs}-T_0)/(T_w-T_0)$
x	normalised axial co-ordinate (z/R)

Greek symbols

α	axial scaling factor
ε	bed voidage
ϕ_i	cubic Hermite basis function
ψ_i	cubic Hermite basis function
θ	dimensionless bed temperature, $(T_b-T_0)/(T_w-T_0)$
μ	viscosity of fluid (kg/ms)
ρ	density of fluid (kg/m^3)
ξ	a general independent variable

References

1) Hiby, J. W., Inst. Chem. Eng. Symp. Series No 9 (1962).

2) Roemer, G., Dranoff, J. S. and Smith, J. M., I.E.C. Fund. 1, 284 (1962).

3) Gunn, D. J. and Khalid, M., Chem. Eng. Sci. 30, 261 (1975).

4) Dixon, A. G., Ph.D. Thesis, University of Edinburgh (1978).

5) Dixon, A. G., Cresswell, D. L. and Paterson, W. R., A.C.S. Symposium Series No 65, (1978).

6) De Wasch, A. P. and Froment, G. F., Chem. Eng. Sci. 27, 5667 (1972).

7) Li, Chi-Hsuing and Finlayson, B. A., Chem. Eng. Sci. 32, 1055 (1977).

8) Young, L. C. and Finlayson, B. A., I.E.C. Fund. 12, 412 (1973).

9) Mears, D. E., I.E.C. Fund. 15, 20 (1976).

10) Hinduja, M. J., Sundaresan, S. and Jackson, R., AIChE J. 26, 274 (1980).

11) Stewart, W. E. and Sørensen, J. P., Proceedings 2nd ISCRE, Amsterdam (1972): (B8) 75-88.

12) Villadsen, J. V. and Stewart, W. E., Chem. Eng. Sci. 22, 1483 (1967); 23, 1515 (1968).

13) Jutan, A., Tremblay, J. P., MacGregor, J. F. and Wright, J. D., AIChE J. 23, 732 (1977).

14) de Boor, C., "A Practical Guide to Splines", Springer-Verlag, Berlin, 1978.

15) Carey, G. F. and Finlayson, B. A., Chem. Eng. Sci. 30, 587 (1975).

16) Prenter, P. M. and Russell, R. D., SIAM J. Numer. Anal. 13, 923 (1976).

17) Paterson, W. R., Dixon, A. G. and Cresswell, D. L., paper 3 in "Computers in Chemical Engineering. Recent Developments in Education and Practice", Meeting of Inst. of Chem. Eng. (Scottish Branch) Edinburgh 1977.

18) Paspek, S. C. and Varma, A., Proc. ISCRE 6, Nice (1980).

19) Dixon, A. G. and Cresswell, D. L., AIChE J. 25, 663 (1979).

20) Prenter, P. M., "Splines and Variational Methods", Wiley Interscience, New York, (1975).

21) Villadsen, J. V. and Michelsen, M. L., "Solution of Differential Equation Models by Polynomial Approximation", Prentice-Hall, Englewood Cliffs, NJ, (1978).

22) Martin, R. S. and Wilkinson, J. H., Numer. Math. 9, 279 (1967).

23) Hopkins, T. and Wait, R., Int. J. Numer. Meth. Eng. 12, 1081 (1978).

24) Guertin, E. W., Sørensen, J. P. and Stewart, W. E., Computers and Chemical Engineering 1, 197 (1977).

25) Birnbaum, I. and Lapidus, L., Chem. Eng. Sci. 33, 455 (1978).

26) Verhoff, F. H. and Fisher, D. P., Trans. ASME, J. Heat Transfer 95, 132 (1973).

27) Russell, R. D. and Christiansen, J., SIAM J. Numer. Anal. 15, 59 (1978).

28) Littmann, H., Barile, R. G. and Pulsifer, A. H., IEC Fund. 7, 554 (1968).

29) Olbrich, W. E., Proc. 'CHEMECA' '70 Conf., Melbourne and Sydney, August 19-26 (1970), p. 101, Butterworth, London (1971).

30) Zehner, P. and Schlünder, E. U., Chemie-Ing.-Techn. 42, 933 (1970).

31) Kunii, D., Suzuki, M. and Ono, N., J. Chem. Eng. Japan 1, 21 (1968).

32) Hsiang, T. C. and Haynes, H. W. Jr., Chem. Eng. Sci. 32, 678 (1977).

Appendix: computational details

For collocation at the Gaussian points within a subinterval, the vectors $\underline{a}_{ij}$, $\underline{b}_{ij}$, $\underline{c}_{ij}$ depend only on h_i and are given by

$$\underline{a}_{i1} = [\frac{1}{2} + \frac{2}{3\sqrt{3}},\ (1 + \frac{1}{\sqrt{3}})\frac{h_i}{12},\ \frac{1}{2} - \frac{2}{3\sqrt{3}},\ (\frac{1}{\sqrt{3}} - 1)\frac{h_i}{12}]$$

$$\underline{a}_{i2} = [\frac{1}{2} - \frac{2}{3\sqrt{3}},\ (1 - \frac{1}{\sqrt{3}})\frac{h_i}{12},\ \frac{1}{2} + \frac{2}{3\sqrt{3}},\ (-1 - \frac{1}{\sqrt{3}})\frac{h_i}{12}]$$

$$\underline{b}_{i1} = [-\frac{1}{h_i},\ \frac{1}{2\sqrt{3}},\ \frac{1}{h_i},\ -\frac{1}{2\sqrt{3}}]$$

$$\underline{b}_{i2} = [-\frac{1}{h_i},\ -\frac{1}{2\sqrt{3}},\ \frac{1}{h_i},\ \frac{1}{2\sqrt{3}}]$$

$$\underline{c}_{i1} = [-\frac{2\sqrt{3}}{h_i^2},\ \frac{-\sqrt{3} - 1}{h_i},\ \frac{2\sqrt{3}}{h_i^2},\ \frac{1 - \sqrt{3}}{h_i}]$$

$$\underline{c}_{i2} = [\frac{2\sqrt{3}}{h_i^2},\ \frac{\sqrt{3} - 1}{h_i},\ -\frac{2\sqrt{3}}{h_i^2},\ \frac{\sqrt{3} + 1}{h_i}] \quad .$$

These vectors are supplied by a FORTRAN subroutine:

CALL BASWTS (ID, H, V) .

This subroutine computes the weights for $u^{(ID)}(x_{i1})$ and $u^{(ID)}(x_{i2})$; i.e. ID is an indicator-variable set to 0,1 or 2 for the function or its' first or second derivative respectively. The length of the subinterval containing x_{i1} and x_{i2} is supplied to the subroutine in H, and the weights are output in the 2×4 array V in the form e.g.

$$\begin{bmatrix} (\underline{a}_{i1}) \\ (\underline{a}_{i2}) \end{bmatrix}$$

for ID = 0, and similarly for ID = 1,2.

The use of these methods to discretise boundary value problems results in a system of algebraic equations

$$A\underline{u} = F(\underline{u})$$

where $\underline{u}$ is the vector of unknowns. The matrix A corresponds to the linear part of the differential operator (and may be $\equiv 0$). If the entire problem is linear then $F(\underline{u})$ reduces to a constant, $\underline{b}$, and solution is straight-forward; otherwise iterative methods must be used. Computational advantage may be taken of the fact that A is a band matrix if the equations are ordered naturally, some thought may have to be given to the placement of the boundary equations to obtain minimum bandwidth.

The band matrix A, of order N with M1 subdiagonal elements and total bandwidth MT, is stored as an $N \times MT$ array. The matrix is factorised in the form $A = LU$, the lower triangle being stored in array XM and the upper overwriting A, by the subroutine BANDET; subroutine BANSOL is then called to solve the banded system $LU\underline{u} = \underline{b}$. The routines are simplications of those given in (22), where further details on the storage method are given.

Once the vector $\underline{u}$ has been obtained, the solution at arbitrary x is found using the formula

$$u(x) = (\underline{a}_i(x) \cdot \underline{u}_i)$$

where $x_i < x < x_{i+1}$.

The vector $\underline{a}_i(x)$ is given by the subroutine

CALL INTWTS(ID,X,XI,XJ,VECT) with ID = 0 ;

x is supplied in X, x_i in XI and x_{i+1} in XJ. Then on output VECT is the 4-vector $a_i(x)$.

If $\underline{b}_i(x)$ is required, INTWTS is called with ID = 1; ID = 2 gives $\underline{c}_i(x)$.

Note BASWTS is a special form of INTWTS where advantage is taken of the need to obtain weights only at the Gaussian points of each subinterval.

It is easy to see that the elements in $\underline{a}_{ij}(y,x)$, $\underline{a}_{i,j+1}(y,x)$, $\underline{a}_{i+1,j}(y,x)$ and $\underline{a}_{i+1,j+1}(y,x)$ may be generated from those in $\underline{a}_i(y)$ and $\underline{a}_j(x)$. Hence $\underline{A}_{ij}(y,x)$ may also be generated from $\underline{a}_i(y)$ and $\underline{a}_j(x)$ and the product o is defined by

$$\underline{A}_{ij}(y,x) = \underline{a}_i(y) \circ \underline{a}_j(x) \quad .$$

Similar relations hold for $\underline{B}^y_{ij}(y,x)$ etc. More generally a 16-element vector VC may be generated from any two 4-element vectors VA and VB via the o-product, and a subroutine to do this is: CALL OPROD(VA,VB,VC).

Collocation within subrectangle ij requires $\underline{A}_{ijk\ell}$ for $k,\ell = 1,2$ given $\underline{a}_{ik}$ and $\underline{a}_{j\ell}$ for $k,\ell = 1,2$. Subroutine PRDWTS calls OPROD four times to achieve this; a typical calling sequence is e.g. to obtain weights for $\frac{\partial^2 \theta}{\partial y^2}$ on subrectangle ij

```
CALL   BASWTS (2,HI,VI)
CALL   BASWTS (0,HJ,VJ)
CALL   PRDWTS (VI,VJ,VYY) .
```

Here VI and VJ are 2×4 matrices as described above and VYY is a 4×16 matrix

$$\begin{pmatrix} (\underline{C}^{yy}_{ij11}) \\ (\underline{C}^{yy}_{ij21}) \\ (\underline{C}^{yy}_{ij12}) \\ (\underline{C}^{yy}_{ij22}) \end{pmatrix} .$$

```
      SUBROUTINE BANDET(ND,N,MTD,MT,M1D,M1,A,XM,IP,IV,IFAIL)
      IMPLICIT DOUBLE PRECISION (A-H,O-Z)
      DIMENSION  IP(ND),A(ND,M1D),XM(ND,M1D)
      IFAIL = 0
      L = M1
      DO 30  I = 1,M1
      IJ = M1 + 2 - I
      DO  25  J = IJ,MT
   25 A(I,J-L) = A(I,J)
      L = L - 1
      JL = MT - L
      DO  30  J = JL,MT
   30 A(I,J) = 0
      L = M1
      DO  100  K = 1,N
      X = A(K,1)
      I = K
      IF  (L.LT.N) L = L + 1
      IF  (K+1.GT.L) GO TO 40
      IK = K + 1
      DO 35 J = IK,L
      IF (DABS(A(J,1)).LE.DABS(X)) GO TO 35
      X = A(J,1)
      I = J
   35 CONTINUE
   40 IP(K) = I
      IF (X.NE.0) GO TO 50
      IFAIL = 1
      IV = K
      RETURN
   50 IF (I.EQ.K) GO TO 70
      DO 65 J = 1,MT
      X = A(K,J)
      A(K,J) = A(I,J)
   65 A(I,J) = X
   70 IF (K+1.GT.L) GO TO 100
      IK = K+1
      DO 90 I = IK,L
      XM(K,I-K) = A(I,1)/A(K,1)
      X = XM(K,I-K)
      DO 80 J = 2,MT
   80 A(I,J-1) = A(I,J) - X*A(K,J)
   90 A(I,MT) = 0
  100 CONTINUE
      RETURN
      END
```

```
      SUBROUTINE BANSOL(ND,N,MTD,MT,M1D,M1,A,XM,IP,B)
      IMPLICIT DOUBLE PRECISION  (A-H,O-Z)
      DIMENSION A(ND,MTD), XM(ND,M1D),IP(ND),B(ND)
      DO 40 K = 1,N
      I = IP(K)
      IF (I.EQ.K) GO TO 10
      X = B(K)
      B(K) = B(I)
      B(I) = X
   10 IF (L.LT.N) L = L + 1
      IF (K+1.GT.L) GO TO 40
      IK = K+1
      DO 20 I = IK,L
      X = XM(K,I-K)
   20 B(I) = B(I) - X*B(K)
   40 CONTINUE
      L = 1
      DO 70 I1 = 1,N
      I = N+1-I1
      X = B(I)
      IW = I-1
      IF (L.EQ.1) GO TO 65
      DO 60 K = 2,L
   60 X = X-A(I,K)*B(IW+K)
   65 B(I) = X/A(I,1)
      IF (L.LT.MT) L = L+1
   70 CONTINUE
      RETURN
      END

      SUBROUTINE BASWTS(ID,H,V)
      IMPLICIT DOUBLE PRECISION (A-H,O-Z)
      DIMENSION V(2,4)
      S3 = DSQRT(3.0D0)
      IF (ID-1) 1,2,3
    1 V(1,1)=0.5+2.0/(3.0*S3)
      V(1,3)=1.0-V(1,1)
      V(1,2)=(1.0+1.0/S3)/12*H
      V(1,4)=(1.0/S3-1.0)/12*H
      GO TO 4
    2 V(1,1)=-1.0/H
      V(1,3)=-V(1,1)
      V(1,2)=0.5/S3
      V(1,4)=-V(1,2)
      GO TO 4
    3 V(1,1)=-2.0*S3/(H**2)
      V(1,3)=-V(1,1)
      V(1,2)=-(1.0+S3)/H
      V(1,4)=(1.0-S3)/H
    4 J=(-1)**(ID+1)
      V(2,2)=J*V(1,4)
      V(2,4)=J*V(1,2)
      V(2,3) =-J*V(1,1)
      V(2,1)=-J*V(1,3)
      RETURN
      END
```

```
      SUBROUTINE INTWTS(ID,X,XI,XJ,VECT)
      IMPLICIT DOUBLE PRECISION (A-H,O-Z)
      H=XJ-XI
      Z=(X-XI)/H
      Y=(X-XJ)/H
      IF (ID-1) 1,2,3
    1 VECT(3)=(3-2*Z)*Z**2
      VECT(1)=1-VECT(3)
      VECT(4)=H*Y*Z**2
      VECT(2)=H*Z*Y**2
      GO TO 5
    2 VECT(1)=6/H*(Z**2-Z)
      VECT(3)=-VECT(1)
      VECT(4)=Z**2+2*Z*Y
      VECT(2)=2*Z*Y+Y**2
      GO TO 5
    3 VECT(1)=6/H**2*(2*Z-1)
      VECT(3)=-VECT(1)
      VECT(2)=(2*Z+4*Y)/H
      VECT(4)=(4*Z+2*Y)/H
    5 RETURN
      END

      SUBROUTINE PRDWTS(V1,V2,V)
      IMPLICIT DOUBLE PRECISION (A-H,O-Z)
      DIMENSION V1(2,4),V2(2,4),V(4,16),VA(4),VB(4),VV(16)
      IPT=0
      DO 10 J=1,2
      DO 10 I=1,2
      IPT=IPT+1
      DO 15 K=1,4
      VA(K)=V1(I,K)
   15 VB(K)=V2(J,K)
      CALL OPROD(VA,VB,VV)
      DO 10 K=1,16
   10 V(IPT,K)=VV(K)
      RETURN
      END

      SUBROUTINE OPROD(VA,VB,V)
      IMPLICIT DOUBLE PRECISON (A-H,O-Z)
      DIMENSION VA(4),VB(4),V(16)
      JJ=1
      DO 10 J=1,2
      DO 10 I=1,2
      K=2*(I-1)+1
      L=2*(I-1)+1
      V(JJ)=VA(K)*VB(L)
      V(JJ+1)=VA(K+1)*VB(L)
      V(JJ+2)=VA(K)*VB(L+1)
      V(JJ+3)=VA(K+1)*VB(L+1)
   10 JJ=JJ+4
      RETURN
      END
```

SECURITY CLASSIFICATION OF THIS PAGE (When Data Entered)

(12) 44

REPORT DOCUMENTATION PAGE

READ INSTRUCTIONS BEFORE COMPLETING FORM

1. REPORT NUMBER: #2116	2. GOVT ACCESSION NO.: AD-A093630
3. RECIPIENT'S CATALOG NUMBER: (9) Technical	
4. TITLE (and Subtitle): SOLUTION OF PACKED-BED HEAT-EXCHANGER MODELS BY ORTHOGONAL COLLOCATION USING PIECEWISE CUBIC HERMITE FUNCTIONS.	5. TYPE OF REPORT & PERIOD COVERED: Summary Report, no specific reporting period
	6. PERFORMING ORG. REPORT NUMBER
7. AUTHOR(s): (10) G. Dixon Anthony	8. CONTRACT OR GRANT NUMBER(s): (15) DAAG29-80-C-0041 JNSF- ENG76-24368
9. PERFORMING ORGANIZATION NAME AND ADDRESS: Mathematics Research Center, University of Wisconsin 610 Walnut Street Madison, Wisconsin 53706	10. PROGRAM ELEMENT, PROJECT, TASK AREA & WORK UNIT NUMBERS: Work Unit Number 2 - Physical Mathematics
11. CONTROLLING OFFICE NAME AND ADDRESS: See Item 18 below	(11) 12. REPORT DATE: Sep[illegible]1980
	13. NUMBER OF PAGES: 40
14. MONITORING AGENCY NAME & ADDRESS (if different from Controlling Office): (14) MRC-TSR-2116	15. SECURITY CLASS. (of this report): UNCLASSIFIED
	15a. DECLASSIFICATION DOWNGRADING SCHEDULE

16. DISTRIBUTION STATEMENT (of this Report)

Approved for public release; distribution unlimited.

17. DISTRIBUTION STATEMENT (of the abstract entered in Block 20, if different from Report)

18. SUPPLEMENTARY NOTES

U. S. Army Research Office and National Science Foundation
P. O. Box 12211 Washington, D.C. 20550
Research Triangle Park
North Carolina 27709

19. KEY WORDS (Continue on reverse side if necessary and identify by block number)

Orthogonal collocation, elliptic partial differential equations, Hermite functions, heat transfer in packed beds.

20. ABSTRACT (Continue on reverse side if necessary and identify by block number)

Orthogonal collocation using piecewise cubic Hermite functions is used to solve the elliptic partial differential equations arising from pseudo-continuum models of heat transfer in a packed bed. Problems arising from a discontinuity in the wall boundary condition and from the semi-infinite domain of the differential operator are discussed. Comparison is made between the computed solution and experimental results.

DD FORM 1 JAN 73 1473 EDITION OF 1 NOV 65 IS OBSOLETE

UNCLASSIFIED

SECURITY CLASSIFICATION OF THIS PAGE (When Data Entered)

221200